

(2)

AD-A154 093

CRDC-CR-84064

MODIFICATIONS TO SOLA-VOF FOR FLOW DYNAMICS IN SPINNING CYLINDERS

20030115006

by C.W. Hirt
J.R. Campbell

FLOW SCIENCE, INC.
Los Alamos, New Mexico 87544

DTIC FILE COPY

DTIC
ELECTE
MAY 24 1985
S D

B

February 1985

US Army Armament, Munitions & Chemical Command
Aberdeen Proving Ground, Maryland 21010-5423

DISTRIBUTION STATEMENT A
Approved for public release
Distribution Unlimited

5 04 00 0 33

REPRODUCED AT GOVERNMENT EXPENSE

Disclaimer

The findings in this report are not to be construed as an official Department of the Army position unless so designated by other authorizing documents.

Disposition

For classified documents, follow the procedures in DOD 5200.1-R, Chapter IX, or DOD 5220.22-M, "Industrial Security Manual," paragraph 19. For unclassified documents, destroy by any method which precludes reconstruction of the document.

Distribution Statement

Approved for public release; distribution unlimited.

UNCLASSIFIED

SECURITY CLASSIFICATION OF THIS PAGE

REPORT DOCUMENTATION PAGE

1a. REPORT SECURITY CLASSIFICATION UNCLASSIFIED		1b. RESTRICTIVE MARKINGS	
7a. SECURITY CLASSIFICATION AUTHORITY		3. DISTRIBUTION/AVAILABILITY OF REPORT Approved for public release; distribution unlimited.	
7b. DECLASSIFICATION/DOWNGRADING SCHEDULE			
4. PERFORMING ORGANIZATION REPORT NUMBER(S) CRDC-CR-84064		5. MONITORING ORGANIZATION REPORT NUMBER(S)	
6a. NAME OF PERFORMING ORGANIZATION Flow Science, Inc.	6b. OFFICE SYMBOL (if applicable)	7a. NAME OF MONITORING ORGANIZATION	
6c. ADDRESS (City, State, and ZIP Code) Post Office Box 933 1325 Trinity Drive Los Alamos, New Mexico 87544		7b. ADDRESS (City, State, and ZIP Code)	
8a. NAME OF FUNDING/SPONSORING ORGANIZATION CRDC	8b. OFFICE SYMBOL (if applicable) SMCCR-RSP-P	9. PROCUREMENT INSTRUMENT IDENTIFICATION NUMBER 81- DAAG29-81-D-0100	
8c. ADDRESS (City, State, and ZIP Code) Aberdeen Proving Ground, MD 21010-5423		10. SOURCE OF FUNDING NUMBERS	
		PROGRAM ELEMENT NO. 1L16102	PROJECT NO. A71A
		TASK NO.	WORK UNIT ACCESSION NO. WA 05
11. TITLE (Include Security Classification) Modifications to SOLA-VOF for Flow Dynamics in Spinning Cylinders			
12. PERSONAL AUTHOR(S) Hirt, C. W. and Campbell, J. R.			
13a. TYPE OF REPORT Technical	13b. TIME COVERED FROM 82 06 TO 82 12	14. DATE OF REPORT (Year, Month, Day) 1985 February	15. PAGE COUNT 27
16. SUPPLEMENTARY NOTATION COR: Paul D. Fedele, SMCCR-RSP-P, (301) 671-2262			
17. COSATI CODES		18. SUBJECT TERMS (Continue on reverse if necessary and identify by block number)	
FIELD 20	GROUP 04	Centrifugal; Ejection; Rotating; Cylindrical; Fluid Mechanics; Spinning; Dissemination; Liquid Flow; SOLA-VOF	
19. ABSTRACT (Continue on reverse if necessary and identify by block number) This report describes a major extension to the SOLA-VOF computer program, which is described in Los Alamos Scientific Laboratory Report LA-8355, 1980. The modified code now has the capability to treat axisymmetric rotating flows with or without free surfaces and rotating flows of two fluids with a well-defined interface. For efficiency, the original code has also been modified to have a better hydrostatic pressure setup and a new pressure solution algorithm, called SADI, which is a user selectable option. Additionally, several code updates, that correct minor errors or improve accuracy, have been added to this version of SOLA-VOF. The modified code is referred to as SOLA-VOF/CSL in recognition of the <u>Chemical Systems Laboratory</u> , which sponsored this development. <i>referred to as VOF(7)...</i>			
20. DISTRIBUTION/AVAILABILITY OF ABSTRACT <input checked="" type="checkbox"/> UNCLASSIFIED/UNLIMITED <input type="checkbox"/> SAME AS RPT. <input type="checkbox"/> DTIC USERS		21. ABSTRACT SECURITY CLASSIFICATION UNCLASSIFIED	
22a. NAME OF RESPONSIBLE INDIVIDUAL BRENDA C. ECKSTEIN		22b. TELEPHONE (Include Area Code) (301) 671-2914	22c. OFFICE SYMBOL SMCCR-SPS-IR

DD FORM 1473, 84 MAR

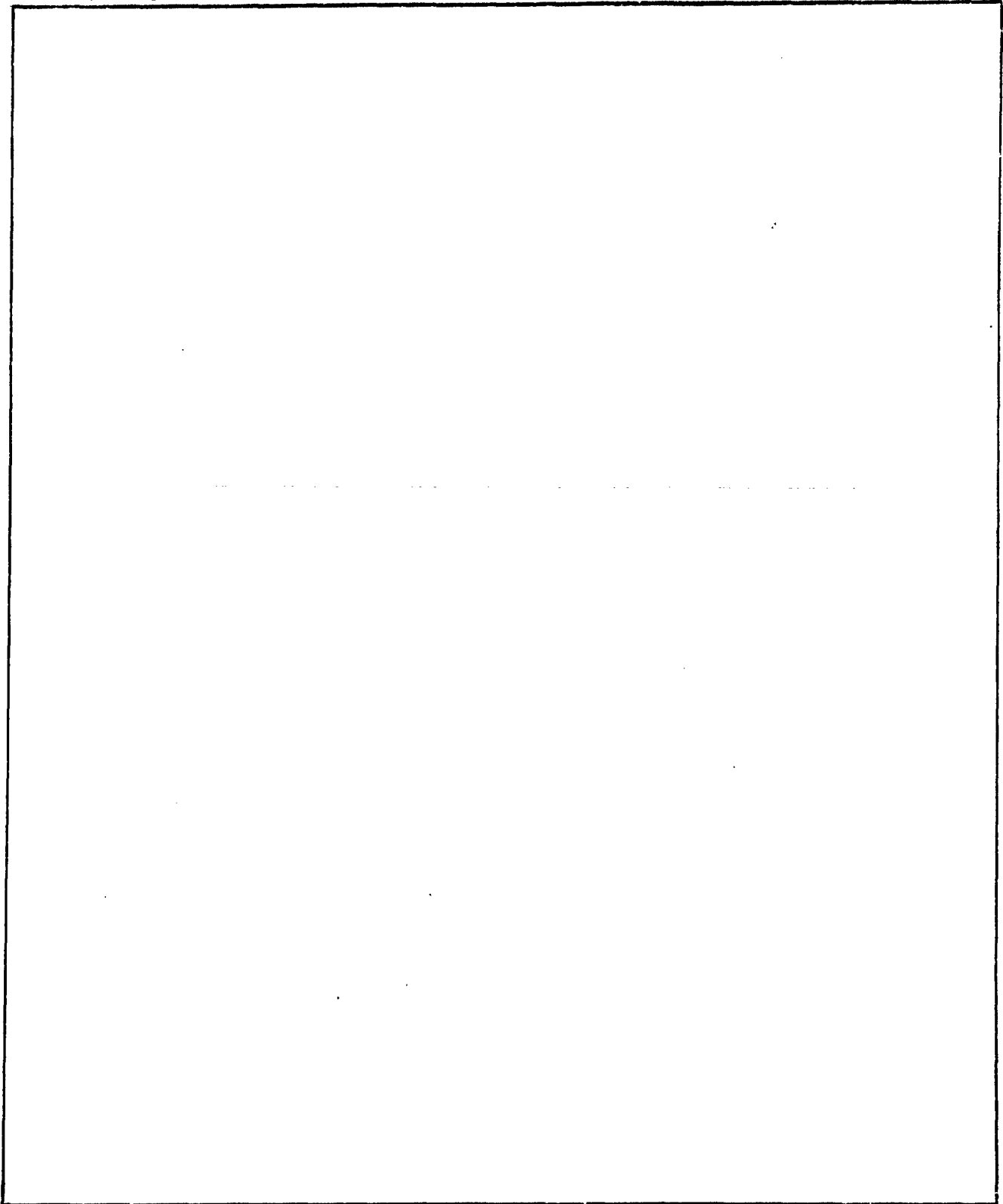
83 APR edition may be used until exhausted.
All other editions are obsolete.

SECURITY CLASSIFICATION OF THIS PAGE

UNCLASSIFIED

A

SECURITY CLASSIFICATION OF THIS PAGE



SECURITY CLASSIFICATION OF THIS PAGE

PREFACE

The work described in this report was authorized under Contract No. DAAG29-81-D-0100. This work was started in June 1982 and completed in December 1982.

The use of trade names in this report does not constitute an official endorsement or approval of the use of such commercial hardware or software. This report may not be cited for purposes of advertisement.

Reproduction of this document in whole or in part is prohibited except with permission of the Commander, US Army Chemical Research and Development Center, ATTN: SMCCR-SPS-IR, Aberdeen Proving Ground, Maryland 21010-5423. However, the Defense Technical Information Center is authorized to reproduce the document for United States Government purposes.

This report has been approved for release to the public.

S DTIC ELECTE **D**
MAY 24 1985
B

Accession For	
NTIS GRA&I	<input checked="" type="checkbox"/>
DTIC TAB	<input type="checkbox"/>
Unannounced	<input type="checkbox"/>
Justification	
Distribution/	
Availability Codes	
Avail and/or	Special
A-1	



Blank

CONTENTS

	Page
1. INTRODUCTION	7
2. THEORY	8
3. NUMERICAL CONSIDERATIONS	9
3.1 Azimuthal Momentum Equation	9
3.2 Implicit Pressure Solution	11
3.3 Miscellaneous Code Changes	12
4. USER INSTRUCTIONS	12
4.1 FLHT and FLHTV	13
4.2 AZW	13
4.3 RPSB and RPSI	13
4.4 IADIX and IADIY	14
4.5 INTDC	14
5. SAMPLE PROBLEMS	14
5.1 Free Surface Example	14
5.2 Two-Fluid Example	19
APPENDIX	23
DISTRIBUTION LIST	29

LIST OF FIGURES

	Page
1 Staggered Mesh	9
2 Initial Fluid Configuration	13
3 Mesh Setup for Example Problems	15
4 Velocity Fields for Example Problem A	16
5 Volume of Fluid in Cylinder Versus Time	17
6 Interface Configuration for Example Problem B	20
7 Velocity Field for Example Problem B	21

Blank

MODIFICATIONS TO SOLA-VOF FOR FLOW DYNAMICS IN SPINNING CYLINDERS

1. INTRODUCTION

Fluid dynamic processes within spinning containers involve many complex phenomena. Boundary layer effects and free surface motions can be strongly coupled with angular momentum effects to produce highly complex flow structures. This situation exists in fluid-filled projectiles. Experimental studies indicate that a better predictive capability is needed to resolve a host of important questions - for instance, how fluid motions affect projectile stability, how spinning fluid is ejected from a projectile with an open end, and how two fluids initially separated within a projectile will mix when the separation device is removed.

The beginnings of a powerful analysis tool that can answer these questions is available in the SOLA-VOF computer program.^{1,2} This program numerically solves the Navier-Stokes equations for an incompressible fluid. Its principal advantage over other programs is its capability for describing the dynamics of fluids with complicated free boundary behavior. Unfortunately, this code does not have provisions for an azimuthal (swirl) velocity component. To remedy this, the project that is described in this report was undertaken to extend SOLA-VOF to have an azimuthal velocity component that could be used in either the one-fluid with free surface or two-fluid with interface cases. The azimuthal velocity addition is also to be compatible with all other capabilities of the original code.

For efficiency, in some calculations we found it necessary to use a new algorithm called SADI for pressure solution. This algorithm is a variant of the well-known Alternating Direction Implicit (ADI) method. SADI is more versatile than ADI, however, because its implicitness can be limited to just the x-direction or just the y-direction. In any case, the method generally converges significantly more rapidly than the standard ADI method.

In the course of this project, we have also included in the new code, SOLA-VOF/CSL, a variety of miscellaneous updates and corrections to the original SOLA-VOF program.

In the next section the theory for incorporating an azimuthal velocity component into SOLA-VOF is briefly described. Then, in Section 3, a discussion is given of the numerical implementation of this theory. Section 4 contains a description of the new input parameters for the code that are required for problems involving rotating fluids. Finally, in Section 5, two sample problems are presented that illustrate the added capabilities.

¹Nichols, B. D., Hirt, C. W., and Hotchkiss, R. S. SOLA-VOF: A Solution Algorithm for Transient Fluid Flow with Multiple Free Boundaries. Los Alamos Scientific Laboratory Report LA-8355. 1980.

²Hirt, C. W., and Nichols, B. D. Volume of Fluid (VOF) Method for the Dynamics of Free Boundaries. *J. Computational Physics* 39, 201 (1981).

2. THEORY

The original SOLA-VOF code was primarily designed for incompressible flow problems governed by the Navier-Stokes equations

$$\frac{\partial u}{\partial t} + u \frac{\partial u}{\partial x} + v \frac{\partial u}{\partial y} = - \frac{1}{\rho} \frac{\partial p}{\partial x} + g_x + \nu \left[\frac{\partial^2 u}{\partial x^2} + \frac{\partial^2 u}{\partial y^2} + \xi \left(\frac{1}{x} \frac{\partial u}{\partial x} - \frac{u}{x^2} \right) \right] \quad (1)$$

$$\frac{\partial v}{\partial t} + u \frac{\partial v}{\partial x} + v \frac{\partial v}{\partial y} = - \frac{1}{\rho} \frac{\partial p}{\partial y} + g_y + \nu \left[\frac{\partial^2 v}{\partial x^2} + \frac{\partial^2 v}{\partial y^2} + \frac{\xi}{x} \frac{\partial v}{\partial x} \right] \quad (2)$$

$$\frac{\partial u}{\partial x} + \frac{\partial v}{\partial y} + \frac{\xi u}{x} = 0. \quad (3)$$

Two dimensional flow is assumed in either plane geometry (x,y) or cylindrical geometry (r,z). The parameter value $\xi = 0$ is the setting for the plane case, while $\xi = 1$ is the setting for cylindrical coordinates (i.e., axisymmetric flow).

A feature of SOLA-VOF that sets it apart from other incompressible flow codes is its ability to treat complex free surface motions (or two-fluid interfaces). This code also contains many user convenient features and has been extensively utilized for a wide range of problems. These aspects of SOLA-VOF make it a highly useful and reliable tool for the analysis of complicated flow problems.

To extend the code for rotating (or swirling) flow, we must add an additional momentum equation governing the azimuthal velocity, w, and a centrifugal acceleration term must be added to the u-equation, Eq. (1). Still assuming axisymmetric flow conditions, the new u- and w-equations are:³

$$\frac{\partial u}{\partial t} + u \frac{\partial u}{\partial x} + v \frac{\partial u}{\partial y} - \frac{\xi w^2}{r} = - \frac{1}{\rho} \frac{\partial p}{\partial x} + g_x + \nu \left[\frac{\partial^2 u}{\partial x^2} + \frac{\partial^2 u}{\partial y^2} + \xi \left(\frac{1}{x} \frac{\partial u}{\partial x} - \frac{u}{x^2} \right) \right] \quad (1a)$$

$$\frac{\partial w}{\partial t} + u \frac{\partial w}{\partial x} + v \frac{\partial w}{\partial y} + \frac{\xi u w}{x} = \nu \left[\frac{\partial^2 w}{\partial x^2} + \frac{\partial^2 w}{\partial y^2} + \xi \left(\frac{1}{x} \frac{\partial w}{\partial x} - \frac{w}{x^2} \right) \right]. \quad (4)$$

³Landau, L. D., and Lifshitz, E. M. Fluid Dynamics. Pergamon Press, London. 1959.

Here we have retained the ξ multiplier on the uniquely cylindrical terms, even though the w-equation has no meaning for azimuthal velocity in the plane geometry case, $\xi = 0$. The reason for this is to maintain flexibility in the basic code so that, for example, the w-equation could still be used for temperature or some other scalar quantity when the code is used for plane coordinate calculations.

The axial momentum equation and the equation for incompressibility are unchanged in the presence of an azimuthal velocity.

Boundary conditions on the azimuthal velocity are $w = w_B$ at a no-slip wall, where w_B is the azimuthal wall velocity. At a free-slip wall there is a zero shear stress, which implies that $\partial w / \partial z = 0$ along a wall normal to the z-axis, while along a cylindrical wall ($r = \text{constant}$) we must have $\partial(w/r) / \partial r = 0$. The code also allows for continuative boundaries, constant pressure boundaries, and periodic boundaries. For continuative and constant pressure boundaries, the free-slip wall conditions are used for the azimuthal velocity as this seems to be the most reasonable choice for these cases.

When free surfaces are present, we have simply assumed that $\partial w / \partial n = 0$, where the derivative is in the direction normal to the surface. For very low Reynolds number flows, say $Re \leq 10$, all the free surface stress conditions used in SOLA-VOF should be revised.^{4,5}

3. NUMERICAL CONSIDERATIONS

3.1 Azimuthal Momentum Equation.

Numerical approximations of Eq. (4) must be made with some care. As noted in the original description of SOLA-VOF,¹ we cannot use a strictly conservative formulation of the advection terms because in a nonuniform mesh our difference approximations would be zeroth order accurate. However, we want to have as close an approximation to the conservative case as possible. The following discussion will illustrate the approach we have taken.

Consider the simple advection problem in conservation form

$$\partial Q / \partial t + \partial uQ / \partial x + \partial vQ / \partial y = 0, \quad (5)$$

where Q is any scalar quantity. We assume a staggered mesh in which Q values are located at centers of mesh cells and velocities are located at cell edges (Figure 1).

⁴Hirt, C. W., and Shannon, J. P. Free Surface Stress Conditions for Incompressible Flow Calculations. J. Computational Physics 2, 403 (1968).

⁵Nichols, B. D., and Hirt, C. W., Improved Free Surface Boundary Conditions for Numerical Incompressible Flow Calculations. J. Computational Physics 8, 434 (1971).

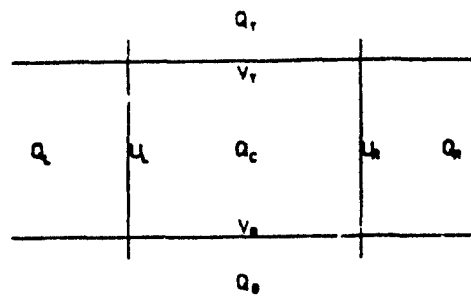


Figure 1. Staggered Mesh

Equation (5) is written in conservative form. The corresponding non-conservative advection equation is

$$\partial Q / \partial t + u(\partial Q / \partial x) + v(\partial Q / \partial y) = 0, \quad (6)$$

where we have assumed the fluid is incompressible,

$$\partial u / \partial x + \partial v / \partial y = 0.$$

Our objective is to write a finite-difference approximation to Eq. (6) that retains at least first-order accuracy in a nonuniform mesh. Furthermore, we would like this approximation to reduce to one for Eq. (5) when the mesh has uniform cell sizes. To do this we begin by writing an approximation to the conservative equation (Eq. 5)

$$(Q_C^{n+1} - Q_C^n) / \delta t + (u_R Q_{DR} - u_L Q_{DL}) / \delta x_C + (v_T Q_{DT} - v_B Q_{DB}) / \delta y_C = 0 \quad (7)$$

where superscripts refer to time levels and δx_C and δy_C are the width and height of the cell (see Fig. 1 for definitions of the subscript notation). Here the Q values chosen for fluxing across each cell boundary are weighed between centered and donor (or upstream) values, e.g.,

$$Q_{DR} = [Q_C + Q_R - \alpha \operatorname{sgn}(u_R)(Q_R - Q_C)] / 2 \quad (8)$$

The case $\alpha = 0$ gives a centered approximation and $\alpha = 1$ the donor cell approximation. The expression $\operatorname{sgn}(u_R)$ means the sign of u_R .

The continuity equation for each cell is

$$(u_R - u_L) / \delta x_C + (v_T - v_B) / \delta y_C = 0 \quad (9)$$

By subtracting Q_C times Eq. (9) from Eq. (7) we find

$$(Q_C^{n+1} - Q_C^n) / \delta t + u_R(Q_{DR} - Q_C) / \delta x_C + u_L(Q_C - Q_{DL}) / \delta x_C + v_T(Q_{DT} - Q_C) / \delta y_C + v_B(Q_C - Q_{DB}) / \delta y_C = 0 \quad (10)$$

This expression is an approximation to Eq. (6). Unfortunately, when the mesh is nonuniform and we select an α value different from zero (which we must for numerical stability reasons) the approximations in Eq. (7), or equivalently Eq. (10), are zeroth order accurate. The reason for this is that the various δx and δy contributions in a Taylor series expansion will combine in such a way as to leave coefficients on the zeroth order advective terms that are different from unity. For instance, the term $u\partial Q/\partial x$ will, for pure donor cell differencing ($\alpha = 1$ and $u > 0$), become

$$u(\partial Q/\partial x)(\delta x_L + \delta x_C)/\delta x_C$$

The ratio of cell sizes is generally zeroth order (it can be first order in special circumstances, depending on the construction of the mesh).

To eliminate this problem we have replaced Eq. (10) by

$$\begin{aligned} (Q_C^{n+1} - Q_C^n)/\delta t + u_R(Q_{DR} - Q_C)/\delta x_{RC} + u_L(Q_C - Q_{DL})/\delta x_{LC} \\ + v_T(Q_{DT} - Q_C)/\delta y_{TC} + v_B(Q_C - Q_{DB})/\delta y_{BC} = 0 \end{aligned} \quad (11)$$

where, e.g., $\delta x_{RC} = (\delta x_R + \delta x_C)/2$. With this small change in the δx and δy divisions we no longer have a strictly conservative approximation (unless the mesh is uniform), but we retain first order spatial accuracy even when $\alpha \neq 0$. Thus, Eq. (11) is the recommended finite-difference approximation for the azimuthal velocity equation, which has been used in SOLA-VOF/CSL.

3.2 Implicit Pressure Solution.

For problems involving fluid motion in spinning cylinders, it is sometimes convenient to use stretched meshes that provide fine zoning near walls to resolve viscous shear stresses. In such cases the mesh will often have some cells with large aspect ratios (i.e. $\delta x \gg \delta y$ or $\delta y \gg \delta x$). When this happens the SOR pressure solution technique used in SOLA-VOF may exhibit extremely slow convergence. To eliminate this problem, we have devised a new solution method based on the Alternating Direction Implicit (ADI) scheme. In the ADI method the pressure on a given row of cells is solved implicitly using a tridiagonal solver. The pressures on adjacent rows are treated as known values and are not changed during this solution step. Each row is treated in this way in a cyclic manner. Then the columns are swept, one-by-one, using a tridiagonal solver for implicitly calculating the pressures in each column. Switching back and forth between rows and columns gives the method its "Alternating Direction" name. If only rows or only columns are implicitly solved, the method is unstable.

Our variation of the ADI method is called SADI. In this scheme we allow some coupling between rows or columns during the one-dimensional implicit solutions. For example, when solving for a row of pressures in the x-direction, one half of the terms representing pressure influences in the y-direction are included. Of course, pressures in neighboring rows are still held fixed. The "one half" prescription has empirically been found to significantly increase convergence of the method. Also, this scheme is stable when only rows or only columns are solved for implicitly. The user selects the desired pressure solution method through the input parameters IADIX and IADIY. When IADIX = 1, rows are treated implicitly; otherwise IADIX should be zero. Similarly for columns, a value for IADIY = 1 gives an implicit solution for columns, and IADIY = 0 otherwise.

As a general rule, the pressure solution should be implicit in the x-direction if there are cells with $\delta x \ll \delta y$ and implicit in the y-direction if there are cells with $\delta y \ll \delta x$.

3.3 Miscellaneous Code Changes.

A calculation of the volume of "F-fluid" in the computing mesh, FVOLT, has been added, and this is printed out with each cycle's short print. F-fluid is the only fluid in a free surface problem, while in a two-fluid problem it is the fluid with density RHOF. FVOLT is also printed at the top of each long print. This bookkeeping feature makes it easy to plot the time history of fluid volume, leaving a cylinder with an open end.

The initial setup routine has been changed so that fluid can be initialized with both vertical and horizontal interfaces. Two input parameters, FLHT and FLHTV, control the fluid distribution. Also, input parameters have been added to assign initial rotation rates to the fluid and to the walls of a cylindrical container. These rates, RPSI and RPSB respectively, are in revolutions per second. All these parameters are described fully in Section 4.

Some corrections have been made to the PETACAL routine. The quantity PETA (I,J) is used as a pressure relaxation factor for full fluid cells that are interpolation neighbors for surface cells. An early update recommended for this factor was not in the CSL version of the SOLA-VOF code. We have added this correction together with a recent modification discovered during the course of this work. These changes should solve the occasional lack of convergence problem encountered in the old code using the SOR pressure solution method. Also, a new calculation for free surface slopes has been included, which works better near boundaries and obstacles.

In a few isolated cases, the P-advection and NF flag setting routines could have occasionally produced spurious results. Although these errors are not likely to cause significant effects in most calculations, we have corrected them in the new code.

4. USER INSTRUCTIONS

SOLA-VOF/CSL is operated in all respects like its predecessor except for the addition of several new input parameters. These parameters are described in the following subsections. A complete list of input parameters is given in the Appendix.

4.1 FLHT and FLHTV.

The initial fluid configuration is defined by these values as indicated in Figure 2. For one material problem the fluid is defined by the $F = 1.0$ region

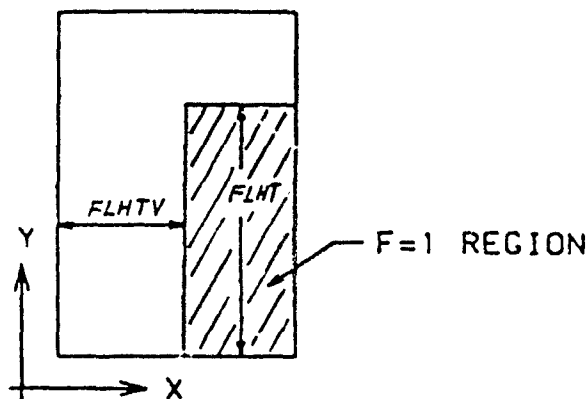


Figure 2. Initial Fluid Configuration

extending in the radial or x-direction from FLHTV to the outer edge of the computing mesh and from the bottom of the computing mesh up to height FLHT. In two material problems the $F = 1.0$ region has density $RHOF$, while the $F = 0.0$ region has density $RHOF_C$. Any other initial fluid configurations must be programmed in the subroutine SETUP. If values for these parameters are not input, they default to $FLHT = 0.0$ and $FLHTV = 0.0$.

4.2 AZW.

A parameter, AZW, is used to indicate when azimuthal velocities are to be computed. If $AZW = 0.0$, the code will run in its original mode and the azimuthal velocity equation will be skipped in the calculations. To select azimuthal velocities, set $AZW = 1.0$. Values of AZW other than 0.0 or 1.0 have no meaning. The default value for AZW is 0.0.

It should be noted that when azimuthal velocities are wanted (i.e., $AZW = 1.0$), the geometry must also be defined as cylindrical, $ICYL = 1$.

4.3 RPSB and RPSI.

Initial fluid and/or container rotation rates can be specified through the parameters RPSB and RPSI. The container or boundary rotation rate in revolutions per second is RPSB. The fluid is given an initial rigid body rotation in revolutions per second equal to RPSI. If there are obstacles defined within the mesh (cells with $BETA = -1.0$), these will receive the rotation RPSI, which will then remain constant in the obstacles throughout a calculation. Boundary rates RPSB will also remain constant unless the user redefines them within the code. When they are not input, these parameters default to zero.

4.4 IADIX and IADIY.

To select the original SOR pressure solution scheme, the values $IADIX = IADIY = 0$ should be input to the code (these values are also the default values). Implicit calculations for pressure will be performed in the x-direction if $IADIX = 1$ and in the y-direction if $IADIY = 1$. Both parameters may be set to unity for the full SADI-type of alternating direction method. If either parameter is different from zero, the over-relaxation parameter OMG will have no effect as it is not used in SADI.

Caution: the SADI scheme will not work with periodic boundary conditions. Periodic boundaries require a more complex solution strategy, which has not been implemented in SOLA-VOF/CSL. SADI, however, will work with any combination of free boundaries and interior obstacles.

4.5 INTDC.

This Parameter controls the difference approximation used in advecting the F-function that defines free surfaces and fluid interfaces. In free surface applications, the advection scheme should use an acceptor-cell type of approximation in the interior of $F = 1.0$ regions. This is insured by setting $INTDC = 0$.

For two-fluid applications, it is usually best to use a donor-cell approximation in the interior F regions. This is obtained by setting $INTDC = 1$. The correct settings for $INTDC$ are automatically established within the code as a default. Thus, $INTDC$ should only be input when the user wishes to override the default values.

5. SAMPLE PROBLEMS

5.1 Free Surface Example.

As an illustration of the new code's capabilities for computing the flow of fluid leaving a spinning cylindrical container, we have run the following problem. A cylinder of radius $R = 1.0$ and length $L = 3.3$ was initialized with fluid occupying 80% of its volume (20% void). Nondimensional units have been used for convenience. The fluid and cylinder are initially in solid body rotation at 92 revolutions per time unit. No axial gravity was assumed so that the fluid has a free surface parallel to the axis of the cylinder. At time zero the top of the cylinder has been instantaneously raised by 0.7 distance units. A constant pressure boundary condition is assumed at the outer radius in the gap formed when the top was raised. Figure 3 shows the mesh setup used for this problem. Figure 4 contains several velocity plots obtained in the course of the calculation. A plot of the volume of fluid contained in the cylinder versus time is given in Figure 5. This problem took a little less than 10 minutes on a CDC-750 computer.

For new users the following discussion will clarify how the code was set up to perform this calculation. The finite-difference mesh must be constructed for the cylinder with raised top and to have only a portion of the $r = R$ boundary open for outflow. The easiest way is to set the right-hand boundary condition as a specified pressure boundary and to define obstacle cells in the right-most column of cells over that portion of the boundary that represents the cylinder wall. The remaining cells in that column (above the obstacle) will then have

I	XL	XC	XR	NXL	NXR	DXMIN
1	0.000	0.050	1.000	7	3	0.350
J	YL	YC	YR	NYL	NYR	OYMIN
1	0.300	0.500	4.000	5	25	0.120
K	X(K)	Y(K)				
1	0.000	0.000				
2	0.103	0.100				
3	0.362	0.200				
4	0.597	0.300				
5	0.620	0.400				
6	0.726	0.500				
7	0.800	0.600				
8	0.850	0.700				
9	0.900	0.800				
10	0.950	0.900				
11	1.000	1.000				
12		1.150				
13		1.270				
14		1.303				
15		1.520				
16		1.650				
17		1.700				
18		1.020				
19		2.060				
20		2.233				
21		2.350				
22		2.500				
23		2.653				
24		2.810				
25		2.970				
26		3.133				
27		3.300				
28		3.470				
29		3.643				
30		3.820				
31		4.000				

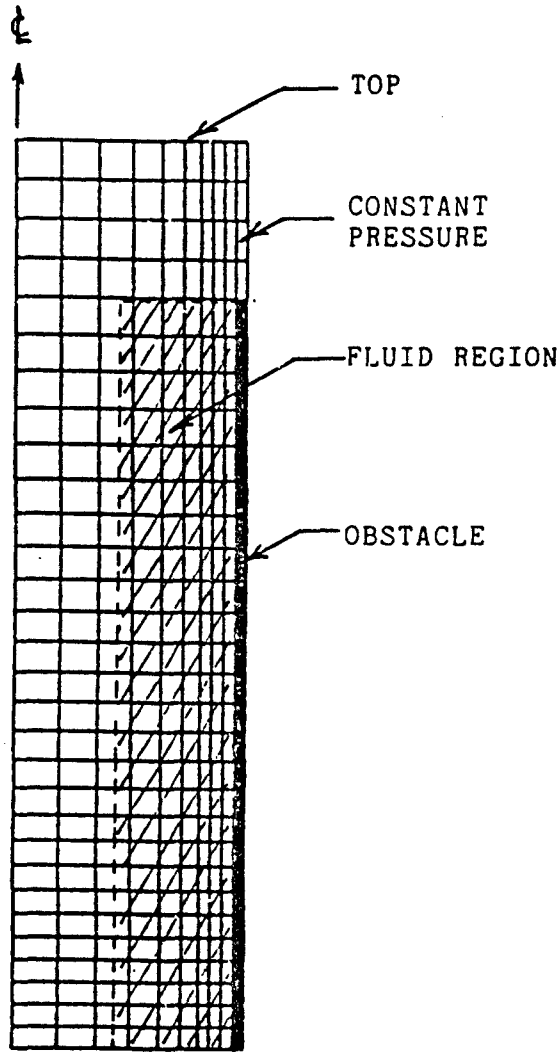


Figure 3. Mesh Setup for Example Problems

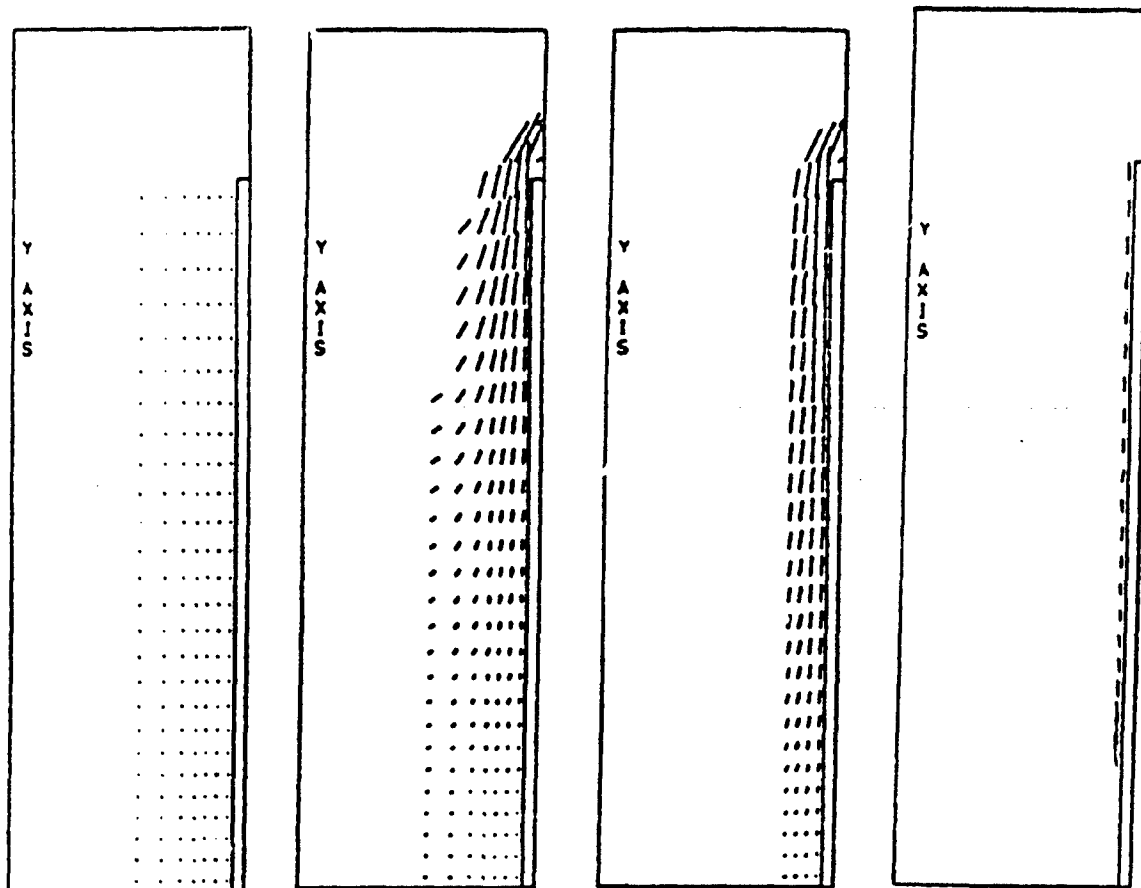


Figure 4. Velocity Fields for Example Problem A

Time (T) and maximum velocity (VM) in each frame is: T = 0.0, VM = 0.0; T = .004, VM = 293; T = .016, VM = 262; T = .089, VM = 37.

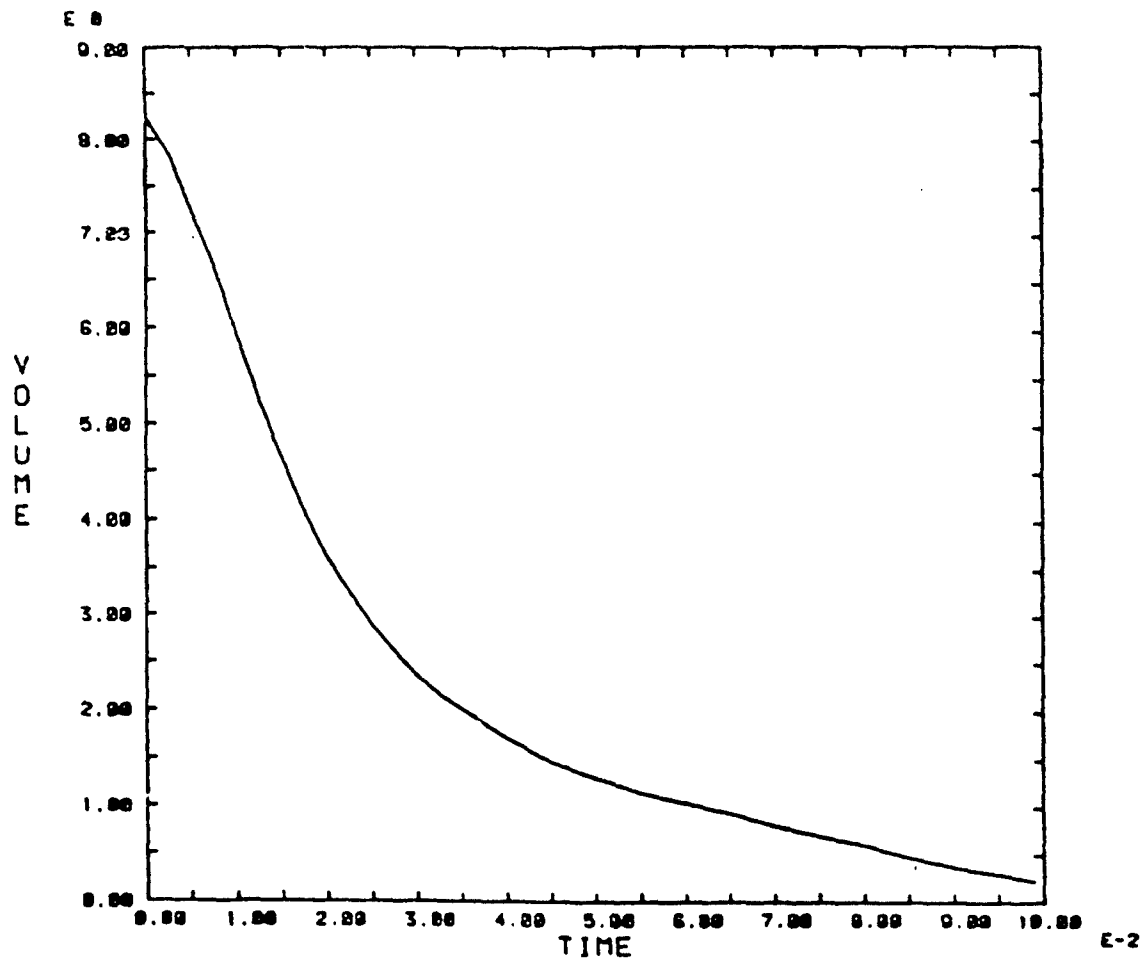


Figure 5. Volume of Fluid in Cylinder Versus Time

the specified outflow boundary pressure, $p = 0$. To account for this obstacle we must define the outer mesh radius to extend one mesh cell further than the radius of the cylinder. Using the automatic mesh generator in the code, we can easily do this by inputting

```
NKX = 1
XL(1) = 0.0   XL(2) = 1.05
XC(1) = 1.0
NXL(1) = 7
NXR(1) = 1
DXMN(1) = 0.05
```

This input assigns $XC(1)$ as the cylinder radius and $XL(2)$ as the radius plus one cell, $NXR(1) = 1$, with width $DXMN(1) = 0.05$. In the sample problem shown in Figure 4, we wanted to have several cells of size 0.05 adjacent to the cylinder wall so we decreased $XC(1)$ and increased the number of cells between $XC(1)$ and $XL(2)$,

```
XC(1) = 0.85
NXR(1) = 4
```

For the axial direction, we wanted small cells at the bottom of the cylinder with uniform stretching toward the top. Thus, we set

```
NKY = 1
YL(1) = 0.0   YL(2) = 4.0
YC(1) = 0.5
NYL(1) = 5
NYR(1) = 25
DYMN(1) = 0.1
```

which puts 5 cells with the minimum height 0.1 at the bottom, and 30 cells altogether to extend the mesh to a maximum height of 4.0. In this problem the height corresponds to the distance between the cylinder's bottom and its top in the raised position. We selected 3.3 as the initial height of the cylinder because this corresponded to the top of cell $j = 27$ in the mesh. Thus, we defined the cylinder wall by setting the last column of cells, $i = 12$, from $j = 2$ to $j = 27$ as obstacle cells, i.e., we set $BETA(i,j) = -1.0$ in these cells. This is done in the SETUP routine.

More generally, to define the vertical mesh so that it will have a mesh line at the top of the cylinder wall, $y = y_{CW}$, and the raised top at $y = y_T$, the y -mesh input should have the form:

```
NKY = 2
YL(1) = 0.0, YL(2) =  $y_{CW}$ , YL(3) =  $y_T$ 
YC(1) =  $y_B$ , YC(2) =  $y_T - y_T$ 
NYL(1) = 1, NYL(2) = ?
NYR(1) = ?, NYR(2) = 1
DYMN(1) =  $y_B$ , DYMN(2) =  $y_T$ 
```

where y_B is the cell size wanted at the bottom wall of the cylinder and y_T is the cell size wanted at the top. The cell numbers $NYL(2)$ and $NYR(1)$ depend on the choices for y_B , y_T , and the overall mesh resolution that the user wants.

To initialize the fluid in the mesh for an 80% fill, we first input FLHT = 3.3 so that the fluid extends up to the top of the closed cylinder. Then FLHTV, which controls the location of the left side of the fluid region, must be calculated to give the 80% fill (or 20% void), i.e., $FLHTV = 0.20R^2$, where R is the cylinder radius. In the present example, FLHTV = 0.4472.

Because we assume an initial solid body rotation the boundary and fluid rotation rates are equal, RPSI = RPSB = 92.

For problems with rotation we must also input AZW = 1.0 and ICYL = 1. The boundary conditions must have WL = 1 because the left boundary is the axis of rotation, WT = WB = 2.0 to have no-slip conditions at the cylinder ends, and WR = 5, which gives the specified pressure condition along that portion of the right boundary that is open for flow. The obstacle along the lower portion of the right boundary defines the cylinder wall and keeps the initial solid body rotation rate assigned to it.

All the remaining input data required for this problem consist of the controls for frequency of output data, time limits, and initial time step. For the initial time step we used 0.0001 as a guess; however, the code cuts this down somewhat as fluid begins to move. We also selected a viscosity of NU = 0.05. This choice was arbitrary and was used only to have non-zero viscous stresses in order to check the code with this option.

5.2 Two-Fluid Example.

As an illustration of a rotating system with two fluids, we have used nearly the same setup as for Example A. Because free surfaces are not allowed when using the two-fluid option, the top of the cylinder has been moved down to a closed position. This is done in the input by defining YL(2) = 3.3 and reducing the cell number NYR(1) from 25 to 21. For consistency we have retained the obstacle cells in column i = 12 and WR = 5. It would be better, in general, to eliminate the obstacle by reducing the mesh in the x-direction to extend only out to the cylinder wall, and using a WR = 2 boundary condition at the right boundary.

The initial fluid configuration consists of a fluid with density 1.0 (RHOF = 1.0) filling the lower half of the cylinder (FLHT = 1.65, FLHTV = 0.0) and a fluid of density 0.9 (RHOFc = 0.9) filling the top half. The system is initially in solid body rotation, RPSI = RPSB = 92. Thus, we envision the fluids having been spun up to a steady state rotation, which requires some sort of diaphragm to keep them from mixing. At the start of our calculation, this diaphragm has been removed and we wish to see how the two fluids will begin to mix.

Figures 6 and 7 show the early fluid interface deformation and velocity fields that were calculated. Initially the heavier fluid on the bottom wants to run up the outer wall into the lighter fluid. This trend only persists for a short time, however, because the large eddy flow associated with this displacement tries to carry fluid near the outer wall inward, and fluid in the inner region outward. Angular momentum carried with this exchange produces an unstable situation and results in complicated, and highly transient, secondary flows. At the time of the last plot, in fact, the inner region has undergone a complete flow reversal. The initial counterclockwise flow has reversed to a large

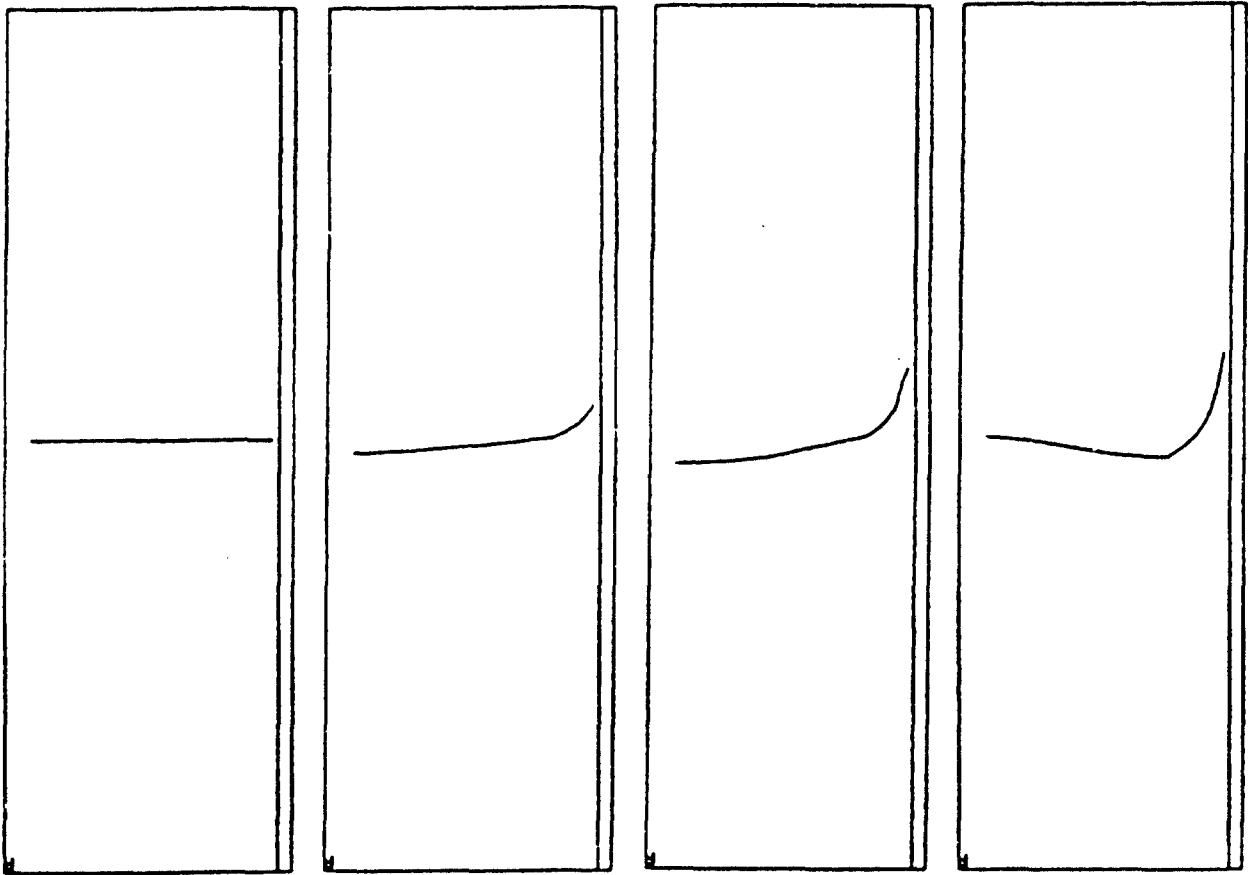


Figure 6. Interface Configuration for Example Problem B at Times:
0.0, .005, .01, and .015

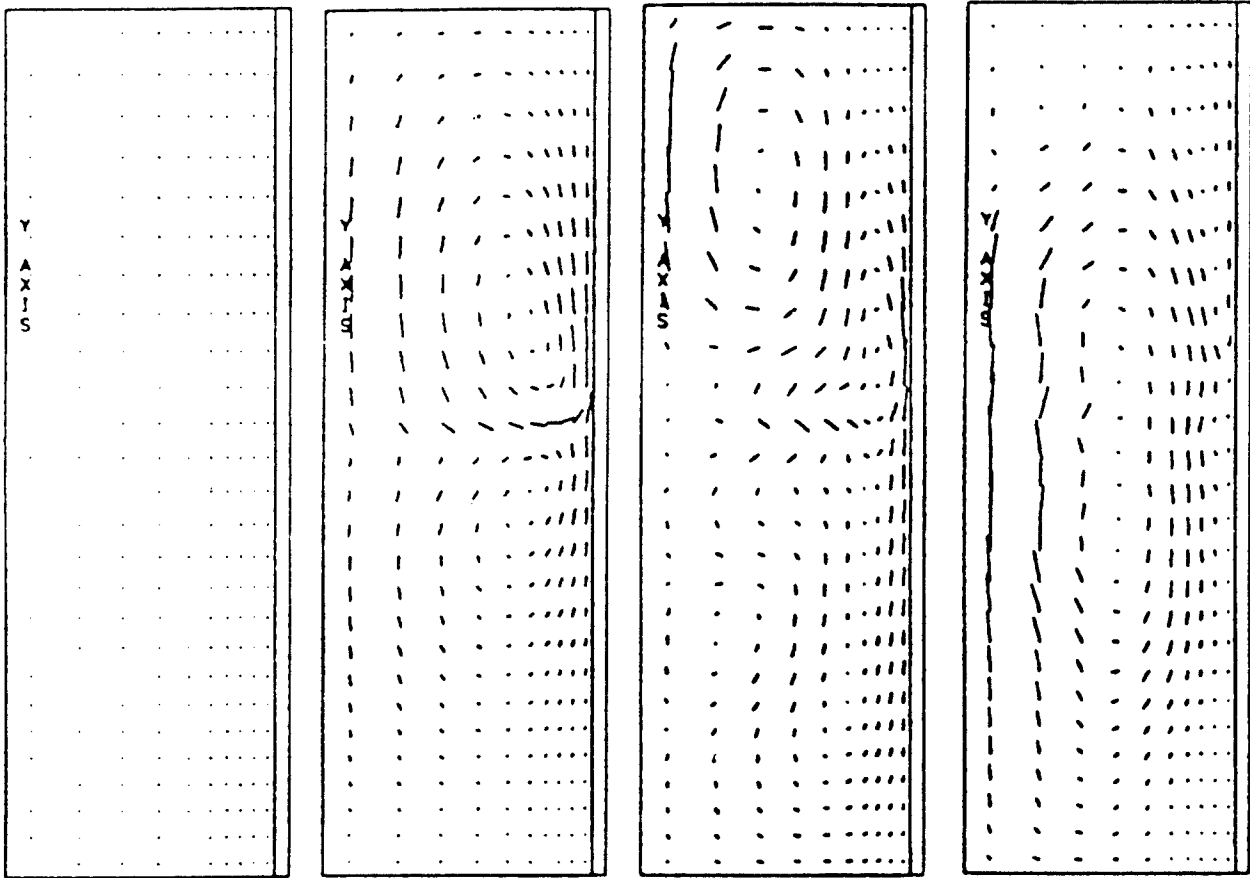


Figure 7. Velocity Field for Example Problem B

Time (T) and maximum velocity (VM) in each frame is: T = 0.0, VM = 0.0; T = .005, VM = 31; T = .01, VM = 26; T = .015, VM = 37.

clockwise eddy extending out to approximately $0.9R$ with a long, narrow counter-clockwise flow along the top portion of the outer wall. With this flow reversal, the fluid interface near the axis is now moving upward.

Approximately 7 minutes of CDC-750 computer time was required to obtain these results. The problem is relatively slow running, probably because of its highly transient character. Lack of funds in our computer budget prevented us from running this problem further. However, it has certainly gone far enough to illustrate this new capability of SOLA-VOF/CSL.

APPENDIX
SOLA-VOF/CSL INPUT DATA

Blank

APPENDIX

SOLA-VOF/CSL INPUT DATA

The following list describes the input data for SOLA-VOF/CSL. Default values are indicated for all quantities. Default values*** indicate quantities that must be specified for each calculation.

NAMelist/XPUT

<u>Quantity</u>	<u>Default</u>	<u>DESCRIPTION</u>
ALPHA	1.0	Controls donor/centered fluxing
AUTOT	1.0	Selects automatic time step control
AZW	0.0	Set to 1.0 for an azimuthal velocity
CANGLE	90	Contact angle in degrees
CSQ	-1.0	Material soundspeed (-1.0=incompressible flow)
DELT	***	Time step size
EPSI	.001	Pressure convergence criterion
FLHT	0.0	Fluid surface in y-direction
FLHTV	0.0	Fluid surface in x-direction
GX	0.0	Body acceleration in x-direction
GY	0.0	Body acceleration in y-direction
IADIX	0	Set to 1 for SADI in x-direction
IADIY	0	Set to 1 for SADI in y-direction
ICYL	0	Set to 1 for cylindrical coordinates
IMOVY	0	Set to 1 for movie output
INTDC	0	Set to 1 for interior F donor cell advection

<u>Quantity</u>	<u>Default</u>	<u>Description</u>
ISURF10	0	Set to 1 for surface tension
ISYMLT	0	Set to 1 for symmetric plot
NMAT	1	Set to 2 for two-fluid applications
NPX	0	Number of particles in x-direction
NPY	0	Number of particles in y-direction
NU	0	Kinematic viscosity
OMG	1.7	Over-relaxation factor
PLTDT	***	Time between plots
PRTDT	***	Time between prints
RHOF	1.0	Density of F=1 fluid
RHOFC	1.0	Density of F=0 fluid
RPSB	0.0	Revolutions per sec of boundary
RPSI	0.0	Revolutions per sec of fluid (initially)
SIGMA	0.0	Surface tension coefficient
TWFIN	***	Problem finish time
UI	0.0	Initial u-velocity
VI	0.0	Initial v-velocity
VELMX	1.0	Scale for velocity plots
WB	1	Bottom boundary condition
WL	1	Left boundary condition
WR	1	Right boundary condition
WT	1	Top boundary condition
XPL	0.0	Left side of particle region

<u>Quantity</u>	<u>Default</u>	<u>Description</u>
XPR	0.0	Right side of particle region
YPB	0.0	Bottom side of particle region
YPT	0.0	Top side of particle region

NAMELIST/MSHSET

DXMN(N)	***	Minimum cell size in x-direction
DYMN(N)	***	Minimum cell size in y-direction
NKX	***	Number of x submeshes
NKY	***	Number of y submeshes
NXL(N)	***	Cells between XL(N) and XC(N)
NXR(N)	***	Cells between XC(N) and XL(N+1)
NYL(N)	***	Cells between YL(N) and YC(N)
NYR(N)	***	Cells between YC(N) and YL(N+1)
XC(N)	***	x coordinate of smallest cell location
XL(N)	***	Left side of submesh N
YC(N)	***	y coordinate of smallest cell location
YL(N)	***	Bottom of submesh N